

Ozone decomposition on the surface of a novel Mn-Al catalyst in gas phase

T. Batakliiev*, V. Georgiev, M. Gabrovska, D. Nikolova, S. Rakovsky

Institute of Catalysis, Bulgarian Academy of Sciences, Acad. G. Bonchev Str. Bl. 11, 1113 Sofia, Bulgaria

Dedicated to the 80th anniversary of Professor Lachezar Petrov, DSc,
Corresponding Member of the Bulgarian Academy of Sciences

Received: November 13, 2019; Revised: January 07, 2020

Ozone is widely used in some industrial and environmental processes as semiconductor manufacturing, deodorization, disinfection, and water treatment. It is a highly toxic gas being harmful regarding human health at concentrations over 0.1 mg/m^3 . An effective method to purge waste gases containing ozone is the catalytic process of heterogeneous decomposition of the latter. The catalytic activity of alumina-supported manganese oxide samples prepared by incipient wetness impregnation was determined by using a specific experimental set-up. Inlet and outlet ozone concentrations were monitored by means of a BMT 964 UV absorption-type ozone analyzer. The catalysts were activated by calcination and their structure characteristics were studied applying physical techniques as BET and TEM. The catalytic properties of the samples were estimated by conversion of a high quantity of dry ozone ($\sim 10000 \text{ ppm}$) to molecular oxygen. It was found that all tested Mn-Al catalysts are active in the ozone decomposition reaction as over 60% conversion was registered for the sample having 15 wt% manganese oxide on the alumina support. The 15-wt% $\text{MnO}_x/\text{Al}_2\text{O}_3$ catalyst exhibited moderate catalytic activity even under humid gas flow conditions measured by the γ coefficient of ozone decomposition. A reaction mechanism of the catalytic ozone decomposition on Mn-Al catalyst was suggested.

Keywords: Ozone decomposition, Manganese catalyst, Impregnation method, Alumina

INTRODUCTION

Ozone is a major air pollutant because of short-term and long-term harm to the human body. Weschler [1] has estimated that ozone exposure of 43–76% occurs indoors and therefore techniques for ozone decomposition need to be developed. The major source of indoor ozone is coming from outdoor ozone [2], while various indoor ozone sources also exist, such as laser printers, photocopiers, and electrostatic precipitators [3–6]. Studies by United States Environmental Protection Agency (US-EPA) on human exposure to air pollutants indicate that the level of many pollutants in indoor air may be two to five times, and occasionally more than 100 times, higher than the level in outdoor air [7]. Commonly used active catalysts for ozone decomposition include noble metals as Au, Pt, and Pd, economically not likable, and transition metal oxides, which are much more cost-effective [8–13]. Manganese oxide catalysts are of great interest due to their excellent redox properties [14] and applicability to many catalytic reactions such as electro-catalytic water oxidation [15], selective oxidation of olefins in the liquid phase [16], and highly effective removal of toluene [17].

Aluminium oxide is well known as catalyst support [18, 19] and recently it has been used in a

manganese oxide containing catalyst system for gas phase decomposition of ozone and nitrogen dioxide in humid indoor air treatment [20]. In another recent study, nitric acid treated birnessite-type MnO_2 has been designed for humid ozone (O_3) decomposition [21]. A sample treated by nitric acid (H-MnO_2) was reported to exhibit a stable O_3 conversion of $\sim 50\%$ within 24 h under 50% of relative humidity and 115-ppm inlet O_3 concentration. The mechanism of ozone destruction process on the surface of alumina-supported silver catalyst has disclosed the important role of the dissociative adsorption of O_3 producing surface chemisorbed atomic oxygen in sufficiently high concentrations to promote oxidation [22]. Silver ability to provide electrons during the reaction and its high concentration on the catalytic surface was reported to initiate the redox chemical reactions thus increasing ozone conversion to molecular oxygen.

The aim of the present study is to investigate the activity of an alumina-supported manganese oxide system during heterogeneously catalyzed ozone decomposition, and to analyze the influence of humidity in the O_3/O_2 gas flow on catalyst efficiency. Finally, an attempt will be made to suggest a catalytic cycle of the ozone decomposition process on the catalyst surface.

* To whom all correspondence should be sent:
E-mail: todor@ic.bas.bg

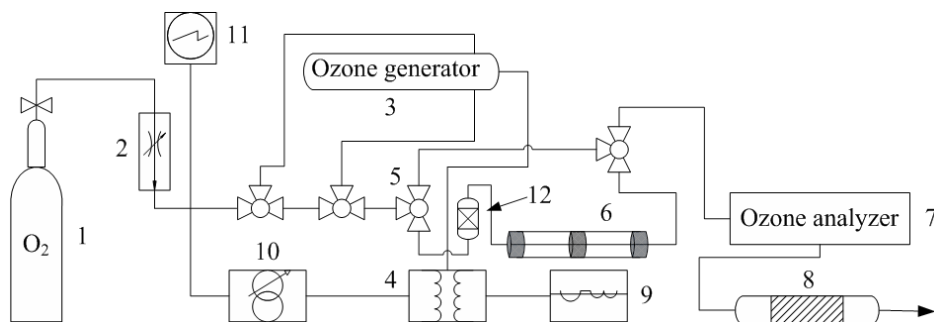


Fig. 1. Experimental set-up for catalytic decomposition of ozone: 1 - oxygen; 2 - flow controller; 3 - ozone generator; 4 - transformer; 5 - three-way stopcock; 6 - reactor charged with catalyst sample; 7 - ozone analyzer; 8 - reactor for decomposition of residual ozone; 9 - current stabilizer; 10 - autotransformer; 11 - voltmeter; 12 - moisturizer.

EXPERIMENTAL

Manganese oxide catalysts (5, 10, and 15 wt%) were synthesized by the incipient wetness impregnation method using aqueous solutions of manganese acetate ($\text{Mn}(\text{CH}_3\text{COO})_2 \cdot 4\text{H}_2\text{O}$, BDH Chemicals >99.99%). Pellet-shaped alumina (Al_2O_3 , BASF, Germany) was employed for catalyst support. After impregnation, the samples were dried at 373 K for 6 h and then calcined at 723 K for 2.5 h to prepare the $\text{MnO}_x/\text{Al}_2\text{O}_3$ catalyst.

Ozone conversion measurements were carried out at room temperature in a tubular glass reactor (10×125 mm) loaded with 0.25 g of catalyst. Figure 1 shows the experimental set-up used for the catalytic tests.

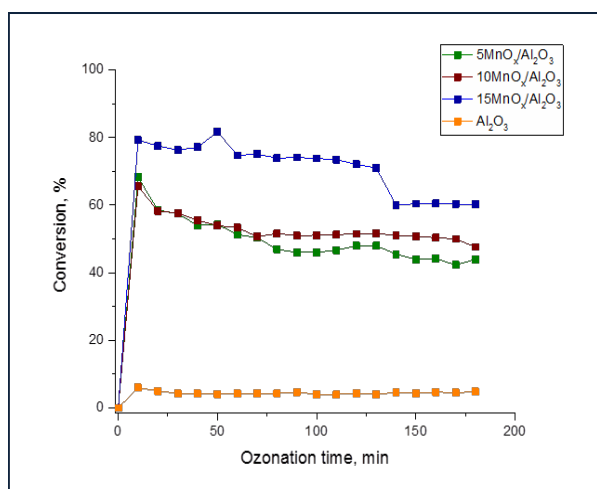


Fig. 2. Ozone conversion as a function of ozonation time for varying manganese oxide contents in the catalyst samples.

Kinetic experiments for determining the catalytic activity in decomposition of dry and humid ozone were performed at O_3/O_2 flow rates ranging from 6.0 to 24 l h^{-1} and inlet ozone concentration of 10000 ppm. The ozone was generated by passing dry oxygen through a high-voltage silent-discharge ozone generator. The inlet and outlet ozone

concentrations were monitored using a BMT 964 UV absorption-type ozone analyzer.

Catalyst textural characteristics were determined by BET (Brunauer-Emmett-Teller) method at a temperature of 77 K using Quantachrome Instruments NOVA 1200, USA. Prior to measurements, the samples were pretreated under vacuum at 200 °C for 2 h. Specific surface area values (S_{BET}) were found by applying BET equation. Pore size (D_{av}) and pore volume (V_t) distributions were calculated from the adsorption branches of the nitrogen physisorption isotherms through BJH method.

Catalyst particle morphology and images of the catalyst crystal lattice were observed by means of high-resolution transmission electron microscopy (HRTEM, JEOL 2100, Japan).

RESULTS AND DISCUSSION

The catalytic activities of titania-supported 5, 10, and 15 wt% manganese oxide samples were compared in the decomposition reaction of ozone produced from pure oxygen under dry conditions (Fig. 2).

The 15-wt% MnO_x catalyst exhibited the highest ozone conversion of almost 80%, in spite of the observed decrease of catalytic activity up to 60% during the last 50 min of reaction time. The catalytic behaviour of the other two samples was very similar showing nearly 50% decomposition of the initial ozone. This was found to be far above the catalytic activity of the unmodified pure alumina used as a support.

As the potential application of the prepared catalysts could be for indoor air treatment, the influence of humid conditions is unavoidable, since a relative humidity between 40 and 65% is mostly encountered in indoor premises [20]. The performance of the Mn-Al catalyst in humid reaction environment was duly compared to the work of a catalyst under dry reaction conditions and was estimated by the γ coefficient of ozone

decomposition (Fig. 3). This coefficient depends on the rate constant of the ozone destruction process and shows catalyst efficiency in the reaction as a count of active interactions (leading to decomposition) of the ozone molecules with the catalyst surface [23]. The definition of γ as an essential ozone decomposition parameter is an important issue of the reaction characterizing the kinetic processes on the interface between solid catalyst surface and O₃/O₂ gas stream. It should be mentioned that studies of materials catalytic activity using the coefficient of ozone decomposition, γ , are applicable when the gas phase reactor has a tubular form. The γ coefficient can be calculated through the following kinetic equation:

$$\gamma = \frac{4\omega}{S_{VT}} \ln \frac{[O_3]_0}{[O_3]}$$

where ω is the O₃/O₂ gas flow rate (l h⁻¹); S - catalyst geometric surface area (cm²); v_T - specific heat rate of ozone molecules (m s⁻¹); [O₃]₀ and [O₃] - inlet and outlet ozone concentrations (ppm), respectively.

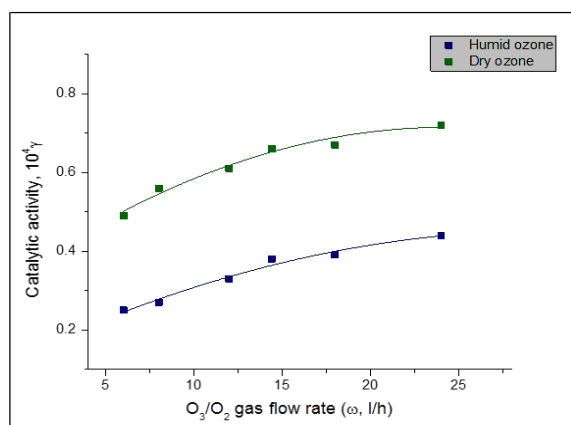
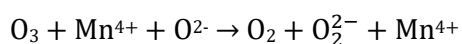


Fig. 3. Flow rate dependence on catalytic activity in dry and humid reaction environment.

As seen in Figure 3, ozone removal efficiency significantly decreases under humid flow conditions but the catalytic performance remains stable and no deactivation was observed. The negative effect of water vapor could be a result of thin film formation on the catalyst surface thus making the ozone diffusion to the active sites more difficult.

An alleged reaction scheme of ozone decomposition consisting of electron transfer from Mn²⁺ catalyst site to ozone molecule is described in Figure 4. The mechanism involves formation of higher oxidation Mn⁴⁺ species generating O₂²⁻ peroxide particles through the redox reaction:



Finally, reduction of the Mn⁴⁺ catalyst site to Mn²⁺ oxidation state occurs upon desorption of a peroxide entity releasing an oxygen molecule (O₂²⁻ → O₂ + 2e⁻). BET specific surface area, pore volume distribution, and average pore size of the catalyst samples are summarized in Table 1. Catalyst textural properties indicate presence of a typical mesoporous structure that can be deduced as well from the nitrogen adsorption-desorption isotherms being of type IV by IUPAC classification. Besides, the hysteresis loop of all catalysts is H2 type, showing a combined mesoporous structure of various size and shape.

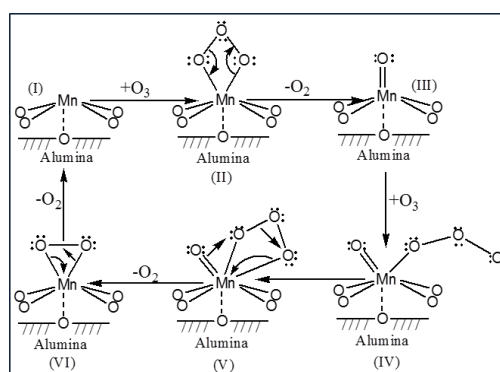


Fig. 4. Mechanism of ozone decomposition on MnO_x/Al₂O₃ catalyst.

Table 1. Textural characteristics of manganese oxide catalysts.

Sample	S _{BET} , m ² /g	V _T , cm ³ /g	D _{av} , nm
Al ₂ O ₃ BASF	253	0.54	8.6
5 wt% MnO _x /Al ₂ O ₃	243	0.52	8.5
15 wt% MnO _x /Al ₂ O ₃	213	0.44	8.3

Isotherm and hysteresis type did not change after modification of the γ-Al₂O₃ support with manganese oxide (Figs. 5a and 5b). The use of incipient wetness impregnation usually leads to catalyst pores filled up by the precursors. Therefore, on comparing the pore structure characteristics of the MnO_x/Al₂O₃ catalyst to the neat γ-Al₂O₃ support one can see a decrease in specific surface area and adsorbed pore volume with increment of manganese content in the samples.

MnO_x/Al₂O₃ catalyst morphology was characterized by HRTEM. Figure 6a is an image of the pure alumina whereas Figure 6b displays well noticeable MnO_x nanocrystalline clusters over the surface of the alumina support. The interplanar spacing of the manganese oxide sample is presented in Figure 6b inset. HRTEM inset image demonstrates catalyst excellent crystallinity suggesting the presence of a tetragonal α-MnO₂ phase with lattice fringe spacing of 0.316 nm corresponding to (310) plane of manganese oxide [9].

Selected area electron diffraction (SAED) patterns are shown in Figures 6c and 6d revealing an improved nanocrystalline state of the manganese

oxide catalyst regarding the unmodified alumina support.

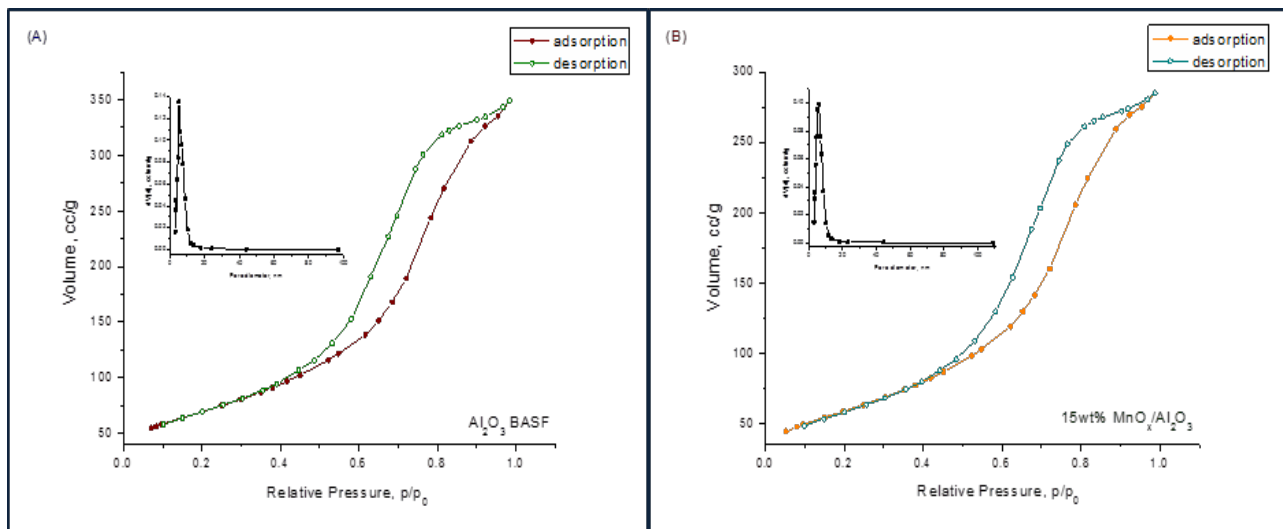


Fig. 5. Nitrogen adsorption-desorption isotherms of pure Al_2O_3 (a) and 15 wt% $\text{MnO}_x/\text{Al}_2\text{O}_3$ catalyst (b)

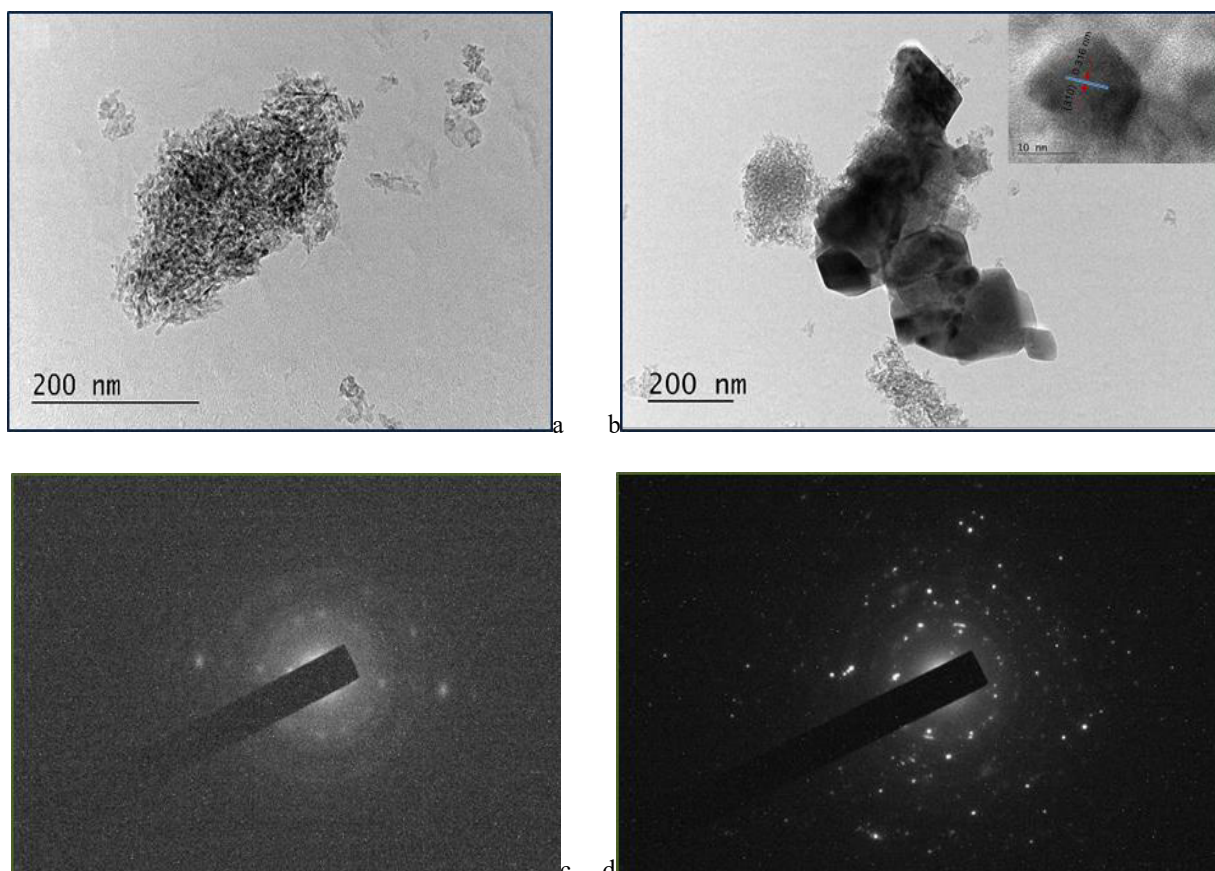


Fig. 6. HRTEM images of Al_2O_3 (a) and $\text{MnO}_x/\text{Al}_2\text{O}_3$ catalyst (b); SAED patterns of Al_2O_3 (c) and $\text{MnO}_x/\text{Al}_2\text{O}_3$ catalyst (d).

CONCLUSIONS

It was found that all analyzed Mn-Al samples show catalytic activity in ozone decomposition reaction as maximum conversion (over 70%) was established for the catalyst having 15 wt% MnO_x. Calculation of γ ozone destruction coefficient at room temperature even under humid reaction environment disclosed that the catalyst keeps moderate performance and did not deactivate under O₃/O₂ gas flow in the range of 6–24 l h⁻¹. The nitrogen adsorption-desorption isotherm of pure alumina is described as typical of mesoporous structure. H₂ hysteresis type did not change after manganese impregnation. TEM images of the catalyst depict excellent nanocrystalline surface morphology of the MnO_x/Al₂O₃ sample.

REFERENCES

1. C. J. Weschler, *Environ. Health Perspect.*, **114**, 1489 (2006).
2. C. J. Weschler, *Indoor Air*, **10**, 269 (2000).
3. T. Tuomi, B. Engström, R. Niemelä, J. Svinhufvud, K. Reijula, *Appl. Occup. Environ. Hyg.*, **15**, 629 (2000).
4. N. Britigan, A. Alshawa, S. A. Nizkorodov, *J. Air Waste Manage.*, **56**, 601 (2006).
5. D. A. Kunkel, E. T. Gall, J. A. Siegel, A. Novoselac, G. C. Morrison, R. L. Corsi, *Build. Environ.*, **45**, 445 (2010).
6. E. Barrese, A. Gioffrè, M. Scarpelli, D. Turbante, R. Trovato, S. Iavicoli, *Occup. Dis. Environ. Med.*, **2**, 49 (2014).
7. R. M. Carver, J. S. Zhang, Z. Wang, Air cleaning technologies for indoor air quality (ACT-IAQ): growing fresh and clean air, New York State Energy Research and Development Authority, 2010, p. 1.
8. Z. P. Hao, D. Y. Cheng, Y. Guo, Y. H. Liang, *Appl. Catal. B: Environ.*, **33**, 217 (2001).
9. G. X. Zhu, J. G. Zhu, W. J. Jiang, Z. J. Zhang, J. Wang, Y. F. Zhu, Q. F. Zhang, *Appl. Catal. B: Environ.*, **209**, 729 (2017).
10. Z. Lian, J. Ma, H. He, *Catal. Commun.*, **59**, 156 (2015).
11. Y. Xiao, X. Wang, W. Wang, D. Zhao, M. H. Qiao, *ACS Appl. Mater. Interfaces*, **6**, 2051 (2014).
12. C. B. Zhang, H. He, K. Tanaka, *Appl. Catal. B Environ.*, **65**, 37 (2006).
13. M. Kobayashi, S. Motonobu, M. Mitsui, K. Kiichiro, *Jap. Pat., CA*, **110**, 120511d (1989).
14. Z. Wu, G. Zhang, R. Zhang, F. Yang, *Ind. Eng. Chem. Res.*, **57**, 1943 (2018).
15. A. C. Thenuwara, E. B. Cerkez, S. L. Shumlas, N. H. Attanayake, I. G. McKendry, L. Frazer, E. Borguet, Q. Kang, R. C. Remsing, M. L. Klein, M. J. Zdilla, D. R. Strongin, *Angew. Chem. Int. Ed.*, **55**, 10381 (2016).
16. R. Ghosh, Y.-C. Son, V. D. Makwana, S. L. Suib, *J. Catal.*, **224**, 288 (2004).
17. F. Wang, H. X. Dai, J. G. Deng, G. M. Bai, K. M. Ji, Y. X. Liu, *Environ. Sci. Technol.*, **46**, 4034 (2012).
18. H. Einaga, S. Futamura, *J. Catal.*, **243**, 446 (2006).
19. F. Lin, Z. Wang, Q. Ma, Y. Yang, R. Whiddon, Y. Zhu, K. Cen, *Appl. Catal. B Environ.*, **198**, 111 (2016).
20. L. Chen, M. Ondarts, J. Outin, Y. Gonthier, E. Gonze, *J. Environ. Sci.*, **74**, 58 (2018).
21. Y. Liu, W. Yang, P. Zhang, J. Zhang, *Appl. Surf. Sci.*, **442**, 640 (2018).
22. T. Batakliiev, G. Tyuliev, V. Georgiev, A. Eliyas, M. Anachkov, S. Rakovsky, *Ozone Sci. Eng.*, **37**, 216 (2015).
23. V. V. Lunin, M. P. Popovich, S. N. Tkachenko, Physical chemistry of ozone, Moscow State University Publisher, 1998 (in Russian).